Statistical Consequences of Toner Size and Charge Distributions

Inan Chen and Ming-Kai Tse; Quality Engineering Associates (QEA), Inc.; Burlington, MA, USA

Abstract

Because of the difference in the nature of forces to separate toners from their carriers, toner samples involved in characterization (e.g. q/m) and in development or transfer process contain distribution of size and charge density different from each other, and from that in a large supply sump. Simulated characterization samples and process samples are created with their respective selection criteria using the Monte Carlo technique. Statistical analyses on the compositions of toner sizes, charges and charge-to-mass ratios in the simulated samples reveal information important in predicting and understanding the performance of electrophotographic toners.

Introduction

Toners for electrophotography (EP) consist of particles of widely distributed sizes and charge densities. Each characterization of toner properties (e.g. charge-to-mass ratio, q/m), or each EP process, such as development and transfer, involves a limited number of toners (i.e., not necessarily covering the full distribution range) separated from their carriers. The "carriers" include magnetic beads, development rollers and photoreceptors (PR). Because of the difference in the nature of separation forces, a preferential selection for certain type of toners can be found in each case. For example, in "blow-off" measurements of q/m,[1] mechanical forces are used to collect the sample toners. The force must overcome the adhesion force (F_a) between toners and carriers. F_a is known to increase with toner size (or radius, r) and surface charge density (σ).[2-4] Hence, toners of smaller r and σ are preferentially selected in these "characterization samples". On the other hand, in development and transfer processes, toner motion is initiated by electrostatic field. The detach field E_d required to free a toner from the carrier bead, roller or PR is known to increase as the toner radius r decreases.[2-4] Thus, toners with larger radii are preferentially found in the developed and/or transferred "process samples". This difference between the contents of characterization and process samples, and from that of supply sump can lead to significant differences in the values of EP parameters (e.g. q/m) and the expected EP performance. Experimental evidence of such preferential selections in process samples has been reported in the literature.[5] The objective of the present work is to quantitatively examine the consequences of such differences by Monte Carlo simulations and statistical analyses of toner parameters in simulated characterization and process samples.

Macroscopic and Microscopic q/m

It is well known that the distribution of toner radius r is log-normal (LN). The distribution of toner surface charge density σ is not well documented, but it is sufficient to assume it to be also LN for the present objective.[6] For a random quantity x (e.g., r or σ) with a LN distribution, the probability density function (PDF), p(x), is given by,

$$p(x) = (1/\sqrt{2\pi}\,\alpha x)\exp\{-[ln(x/\xi)/\alpha]^2/2\} \quad (1)$$

where the median ξ and the deviation α are related to the average x_o and the relative standard deviation (RSD) δ by,[4,7]

$$\xi = x_o/(1+\delta^2)^{1/2} \quad (2a)$$

$$\alpha = [ln(1+\delta^2)]^{1/2} \quad (2b)$$

The average value $\langle x^n \rangle$ of n-th power of x (r or σ) over the full LN distribution ($0 \le x \le \infty$) is given by,[4]

$$\langle x^n \rangle = \int_0^\infty x^n p(x)dx = x_o^n(1+\delta^2)^{n(n-1)/2} \quad (3)$$

The mass m and the charge q of a toner particle can be expressed in terms of r and σ as,

$$m = (4\pi/3)\rho r^3 \quad (4a)$$

$$q = 4\pi r^2\sigma \quad (4b)$$

where ρ is the mass density, which is assumed to have a constant value ($\approx 10^6$ g/m^3) in this work.

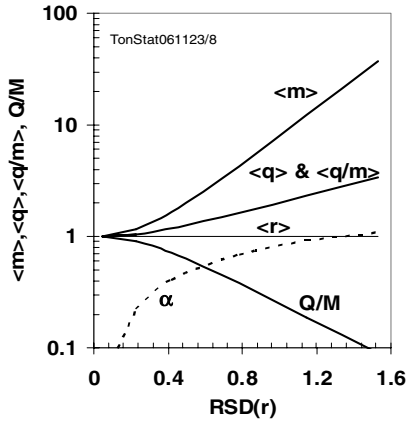

Figure 1. *Dependence of average values of m, q and microscopic q/m, and macroscopic Q/M on RSD δ_r of r distribution (Eqs. 6-8). The relation between α and RSD δ_r (Eq. 2b) is also shown in dashed curve.*

The motion of each toner in EP processes is related to the charge-to-mass ratio of that toner. Using Eq. (4), this ratio, referred to as "microscopic q/m", is given by,

$$q/m = 3\sigma/\rho r \quad (5)$$

For a sample that contains toners covering the full LN ranges of r and σ, the average values <m> and <q> of toner mass m and charge q, respectively, are given from Eqs.(3 and 4) as,

$$\langle m \rangle = m_o(1+\delta_r^2)^3 \quad (6a)$$

$$\langle q \rangle = q_o(1+\delta_r^2) \quad (6b)$$

where δ_r is the RSD of r-distribution, m_o and q_o are the mass and the charge, respectively, of a toner that has the average radius r_o and the average charge density σ_o, namely, $m_o = (4\pi/3)\rho r_o^3$ and $q_o = 4\pi r_o^2\sigma_o$. Similarly, the average value of the microscopic q/m is, from Eqs. (3 and 5),

$$<q/m> = (3\sigma_o/\rho r_o)(1 + \delta_r^2) = (q_o/m_o)(1 + \delta_r^2) \quad (7)$$

In contrast, the charge-to-mass ratio measured by the "blow-off" technique (referred to as "macroscopic Q/M") is given by the ratio of the sum of q's to the sum of m's of toners in the blow-off sample. If the sample contains toners covering the full LN ranges of r and σ, it can be expressed as the ratio of the averages <q> and <m> in Eq. (6). Thus, from Eq. (6) and (7) we have,

$$Q/M = \Sigma q/\Sigma m = <q>/<m> = (q_o/m_o)/(1 + \delta_r^2)^2 \quad (8a)$$

$$= <q/m> /(1 + \delta_r^2)^3 \quad (8b)$$

Figure 1 shows the dependence of the averages and Q/M values (Eqs. 6, 7, 8) on the RSD of r distributions, δ_r. It can be seen that as δ_r (or α_r) increases, the average value of microscopic q/m ratio increases, while the measured (blow-off) macroscopic Q/M decreases. Thus, the difference between the two ratios becomes more significant. It is also noted that these quantities are all independent of the RSD of the surface charge density (σ) distribution.

Adhesion Force and Detach Field

The particle radius (r) and surface charge-density (σ) dependences of toner adhesive force F_a, can be expressed by,[2,3]

$$F_a(r, \sigma) = 4\pi(A_{es}r^2\sigma^2 + A_{ne}r) \quad (9)$$

where the coefficients A_{es} and A_{ne} are empirically determined to be typically $A_{es} \approx 1.6\text{x}10^{11}$ Nm^2/C^2 and $A_{ne} \approx 6.3\text{x}10^{-4}$ N/m for surfaces of EP interests.

In most EP processes, toners are removed from a surface when the electrostatic force, given by the product of toner charge q and the external field, is greater than the adhesion force F_a. Thus, from Eqs. (4 and 9) the required detach field E_d is given by,

$$E_d(r, \sigma) = F_a/q = A_{es}\sigma + A_{ne}/r\sigma \quad (10)$$

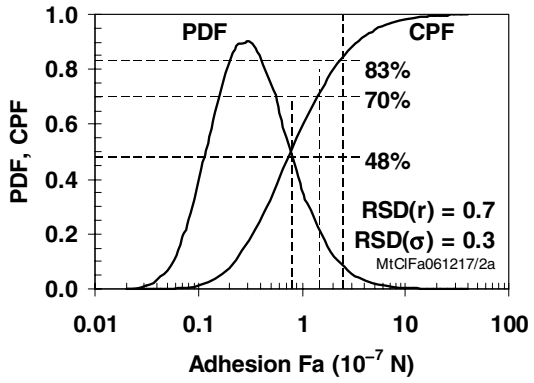

***Figure 2.**. PDF and CPF of adhesion force F_a from LN distributions of r and σ, with averages: r_o = 5 μm, σ_o = 40 μC/m^2, and RSD(r) = 0.7, RSD(σ) = 0.3.*

As mentioned in Introduction, the constituent toners of characterization samples must have r and σ values such that the F_a value (Eq. 9) is smaller than a certain cut-off value F_{mx}. Similarly, the constituent toners of process samples must have r and σ values such that the E_d value (Eq. 10) is smaller than a certain cut-off value E_{mx}. From a supply of a large number of toners (with LN distributions of r and σ) a sample of toners that satisfy the above requirements can be selected by the Monte Carlo simulation technique. Then, the selected sample is statistically analyzed. This includes: the distributions of r, σ and the microscopic q/m ratios, and their averages over the selected sample, as well as the macroscopic Q/M ratio from the sums over the same samples (referred to as "truncated samples").

The simulation procedure is as follows. A set of r and σ values is generated by two independent random number generators. One generates r values that have LN distribution with average r_o and RSD δ_r. The other generates σ values that have LN distribution with average σ_o and RSD δ_s. This set of r and σ is used to calculate m, q, q/m, (Eqs. 4, 5), and F_a or E_d, (Eqs. 9, 10). The toner represented by the set (r, σ) is included in the sample only if $F_a \le F_{mx}$ (for characterization samples) or $E_d \le E_{mx}$ (for process samples). The results with different RSD's and cut-off values, F_{mx} or E_{mx} are compared and discussed in the next section.

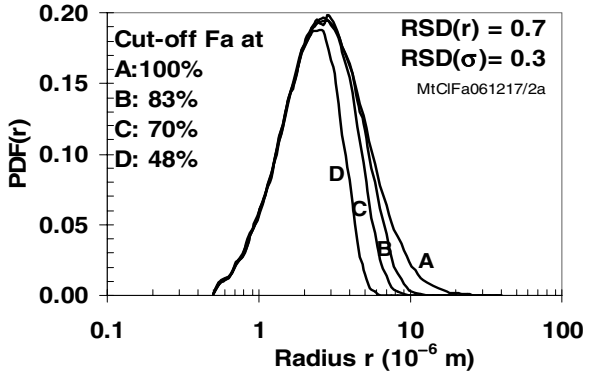

***Figure. 3.** PDF's of r distributions with F_a cut-offs at 100, 83, 70 and 48 % populations, from full LN distributions with r_o = 5 μm, σ_o = 40 μC/m^2, RSD(r) = 0.7, RSD(σ) = 0.3.*

Statistics of Truncated Samples

Figure 2 shows an example of PDF and CPF (cumulative probability function) of F_a distribution,[8] simulated with averages: r_o = 5 μm and σ_o = 40 μC/m^2, and RSD's: δ_r = 0.7 and δ_s = 0.3. The distribution includes full ranges of r and σ, yielding F_a values from 0.01 to >10 (in units of 10^{-7} N). The CPF curve shows that the F_a values chosen (arbitrarily) as the cut-off values F_{mx} = 2.5, 1.5, and 0.8 (x10^{-7}N) to simulate characterization samples in the following figures (Figs. 3 to 5) correspond to 83%, 70% and 48% population, respectively, of lower F_a toners.

The PDF of radius r with the above-mentioned F_a cut-off values are shown in Fig.3. As expected, more of the larger radius toners are excluded from the sample as the F_{mx} value decreases (i.e. the population % decreases). Similar PDF's for σ distributions are shown in Fig. 4. In this case, the exclusion of

toners is not restricted to the higher or the lower values of σ, but more spreads across the range.

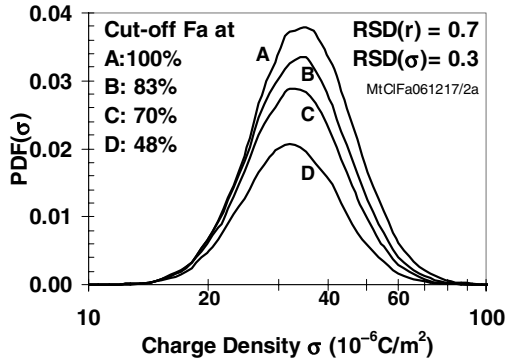

Figure. 4. *PDF's of σ distributions with F_a cut-off corresponding to 100, 83, 70 and 48 % populations, from the same full distributions as in Fig. 3.*

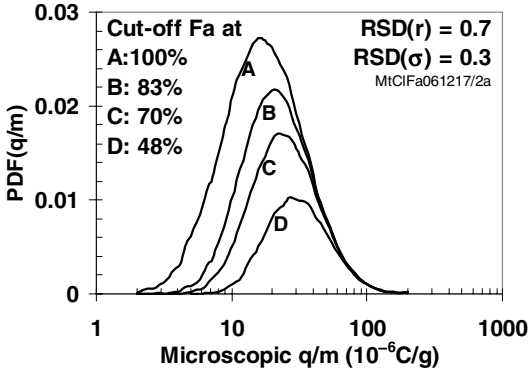

Figure. 5. *PDF's of q/m distributions with F_a cut-offs at 100, 83, 70 and 48 % populations, from the same full distributions as in Fig. 3.*

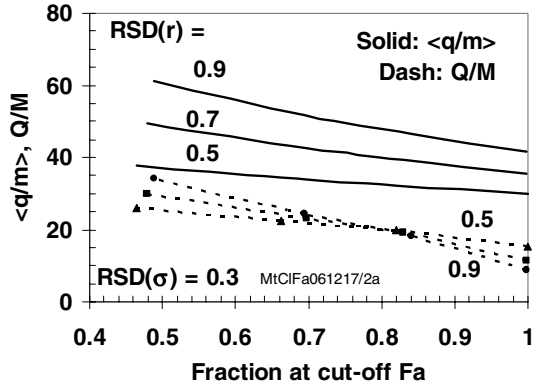

Figure.6*. Average of microscopic q/m (solid curves) and macroscopic Q/M (dashed curves), in units of 10^{-6}C/g, of characterization samples (with cut-off F_a), obtained from full distributions with three RSD(r) values (on figure) and r_o = 5 μm, σ_o = 40 μC/m² and RSD(σ) = 0.3.*

Figure 5 shows the distributions of microscopic q/m ratios with the F_a cut-off values corresponding to the above four populations. It can be seen that as the F_{mx} decreases, more toners with smaller q/m are excluded from the sample, increasing the average value of q/m, as can also be seen in Fig. 6. The latter figure summarizes the results of similar simulations repeated for different values of RSD(r) = δ_r = 0.5, 0.7 and 0.9. It can be seen that both the microscopic average <q/m> and the macroscopic Q/M increase as the F_a cut-off decreases. Furthermore, <q/m> is consistently larger than Q/M at the same cut-off F_a, and the difference increases as RSD(r) increases.

In similar analyses for process samples, a toner is included in the selected sample only if the detach field E_d calculated from a set of random r and σ values is smaller than the cut-off value E_{mx}. An example of PDF and CPF of E_d is shown in Fig. 7. The (arbitrarily chosen) cut-off E_{mx} values corresponding to CPF = 0.81, 0.64, 0.51 are 1.35, 1.15, 1.05 (x10^7 V/m), respectively.

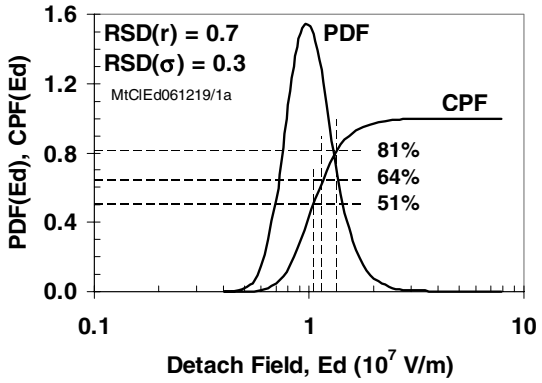

Figure. 7. *PDF and CPF of detach field E_d from LN distributions of r and σ, with r_o = 5 μm, σ_o = 40 μC/m², and RSD(r) = 0.7, RSD(σ) = 0.3.*

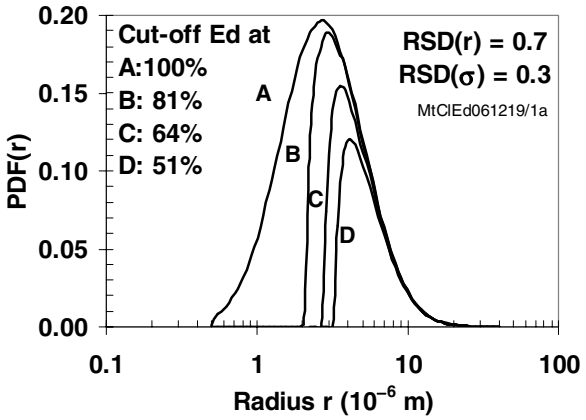

Figure 8. *PDF's of r distributions with E_d cut-offs at 100, 81, 64 and 51 % populations, from full distributions with r_o = 5 μm, σ_o = 40 μC/m², RSD(r) = 0.7, RSD(σ) = 0.3.*

The radius r and the charge density σ distributions for the four sets of cut-off E_d values are shown in Figs. 8 and 9 respectively. Contrary to the case of characterization samples (Fig.3), more toners with smaller radius are excluded from these process samples as the cut-off E_d value decreases (Fig.8). As for charge density distributions (Fig. 9), the exclusion is more spread

over the whole range of σ values, as in the characterization samples (Fig. 4).

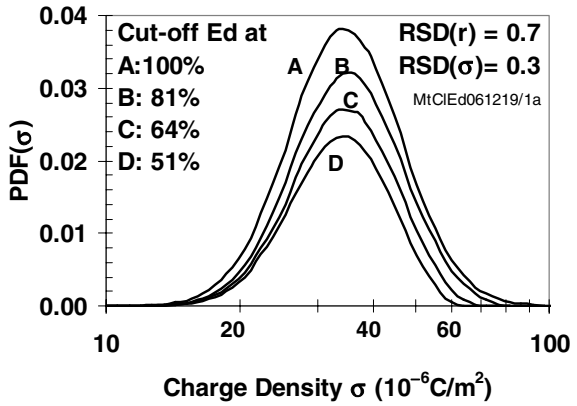

***Figure. 9**. PDF's of charge density distributions with E_d cut-offs at 100, 81, 64 and 51% populations, from the same full distributions as in Fig.8.*

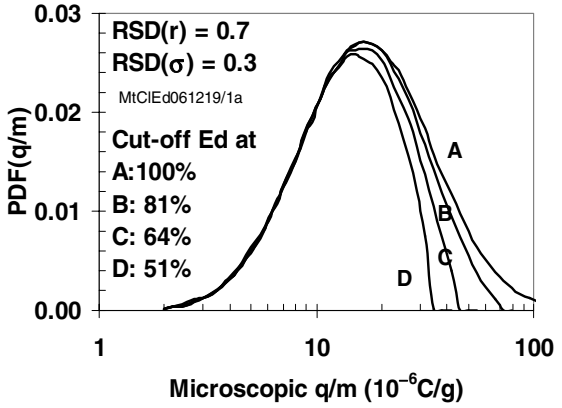

***Figure. 10**. PDF's of microscopic q/m distributions with E_d cut-offs at 100, 81, 64 and 51 % populations, from the same full distributions as in Fig. 8.*

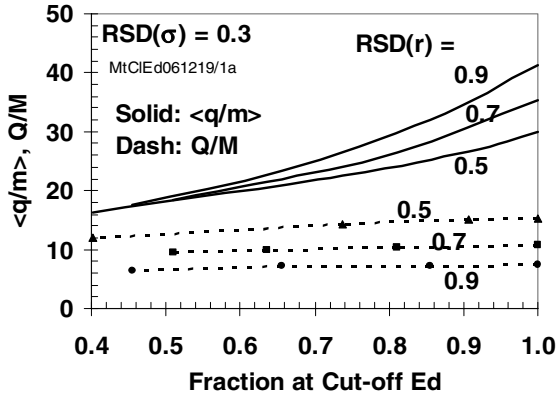

***Figure 11.** Average of microscopic q/m (solid curves) and macroscopic Q/M (dashed curves), in units of 10^{-6}C/g, of process samples (with cut-off E_d) obtained from full distributions with three RSD(r) values (on figure) and r_o = 5 μm, σ_o = 40 μC/m² and RSD(σ) = 0.3.*

The distributions of microscopic q/m ratios in these process samples are shown in Fig. 10. Toners with smaller q/m ratios are preferentially included in these samples, in contrast to the case of characterization samples (Fig. 5). Thus, the average values of q/m in the process samples can be expected to be smaller as the cut-off E_d decreases. This is shown in Fig.11, which includes the results of microscopic average q/m as well as the macroscopic Q/M values obtained with three different RSD(r)'s.

Summary and Conclusions

Truncated characterization and process samples are constructed with the Monte Carlo simulation technique to investigate the statistical nature of the constituent toners. In the characterization samples, toners are selected with the criterion of cut-off adhesion $F_a \leq F_{mx}$. The microscopic average <q/m> and macroscopic Q/M ratios are found to increase as F_{mx} decreases (Fig.6). In the process samples, toners are selected with the criterion of cut-off detach field $E_d \leq E_{mx}$. Both <q/m> and Q/M are found to decrease as E_{mx} decreases (Fig. 11).

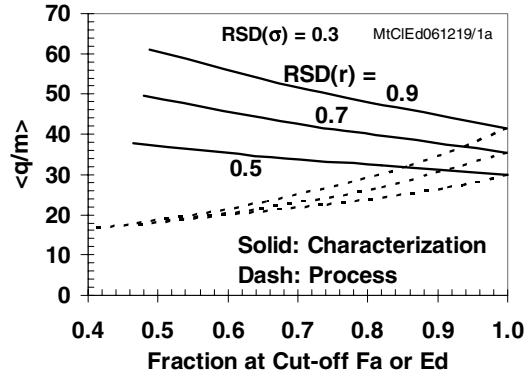

***Figure 12.** Average of microscopic q/m in units of 10^{-6}C/g, of characterization samples (solid curves) and process samples (dashed curves), reproduced from Figs. 6 and 11,respectively.*

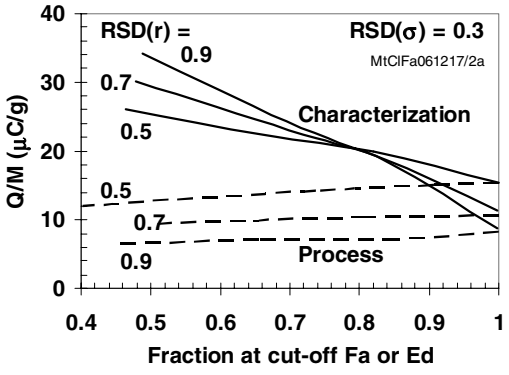

***Figure 13.** Macroscopic Q/M in units of 10^{-6}C/g, of characterization samples (solid curves) and process samples (dashed curves), reproduced from Figs. 6 and 11, respectively.*

The average <q/m> and the macroscopic Q/M shown in Fig. 6 and Fig. 11 are combined and reproduced in Fig. 12 and Fig. 13,

respectively for easier comparison. The difference of <q/m> values (or Q/M values) in the two types of samples can be as much as a factor of two depending on the cut-off value (i.e., population fraction) for the samples, and on the RSD in the supply sump. For example, with the cut-off at 75% population and RSD(r) ≈ 0.7, the characterization sample yields microscopic average <q/m> ≈45 μC/g, while the process sample yields <q/m> ≈ 23 μC/g. The corresponding values for the macroscopic ratio are Q/M ≈ 24 μC/g for the characterization samples and Q/M ≈ 10 μC/g for the process samples.

There is also a significant difference between the macroscopic ratio (Q/M) and the average of microscopic ratio <q/m> in both the full and the truncated distributions, as shown in Fig. 14, which is reproduced from the data in Figs. 6 and 11, for one set of RSD(r) and RSD(σ) only. In case the whole population in the supply sump participates both in characterization and process, it can be shown analytically (in Eq. 8 and Fig. 1) that the average microscopic q/m ratio (effective in EP process) is more than 3 times larger than the macroscopic Q/M ratio (obtained in characterization). In the truncated samples, the difference between the two ratios decreases slightly in both characterization and process samples.

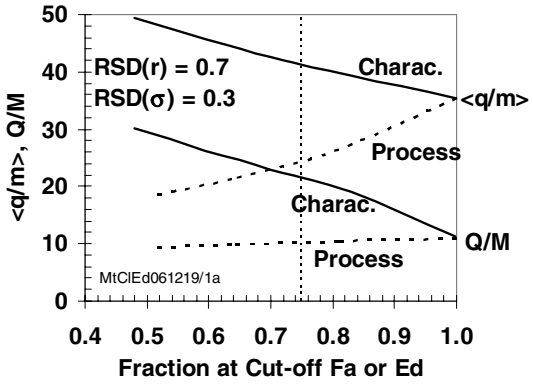

Figure 14. *Macroscopic Q/M and average of microscopic q/m, in units of 10^{-6}C/g, for characterization samples (solid curves) and process samples (dashed curves), reproduced from Figs. 6 and 11, for one set of RSD's (on figure).*

The above conclusions suggest that one should be cautious in using the data from the characterization samples to expect the performance of process samples. The statistical compositions of the samples should be taken into consideration. Alternatively, characterization methods that simulate the processes as much as possible should be considered.

References

[1] T. Oguchi et al., Proc. IS&T's NIP-17, p. 369 (2001)

[2] D. S. Rimai, D. J. Quesnel, L. P. DeMejo, and M. T. Regan, *J. Imaging. Sci. Technol.* **45**, 179 (2001)

[3] J. Hirayama, T. Nagao, O. Ebisu, H. Fukuda and I. Chen, *J. Imaging. Sci. Technol.* **47**, 9, (2003)

[4] I. Chen, Proc. IS&T's NIP-19, pg. 36 (2003)

[5] M. J. Hirsch, Proc. IS&T's NIP-22, pg. 398 (2006)

[6] Essentially the same conclusions are obtained with the assumption that charge density distribution is normal (Gaussian), instead of log-normal.

[7] Relative standard deviation, RSD, is defined as the ratio of standard deviation to the average, see also Ref. 4.

[8] Cumulative probability function, CPF(x) is the integral of PDF p(x) from the minimum to x, approaching unity as x approaches infinity.

Author Biography

Inan Chen received his Ph.D. from the University of Michigan in 1964. He worked at Xerox Research Laboratories in Webster, NY, from 1965 to 1998. Currently, he is a consulting scientist for Quality Engineering Associates (QEA), Inc. and others. He specializes in mathematical analyses of physical processes, in particular, those related to electrophotographic technologies. He is the recipient of IS&T's 2005 Chester F. Carlson Award. Contact at inanchen@frontiernet.net or www.qea.com